Journal of Petroleum
Science and Technology

An Effective EOS Based Modeling Procedure for Minimum Miscibility Pressure in Miscible Gas Injection

Leila Mashayekhi, Mehdi Assareh*, and Norollah Kasiri
School of Chemical Engineering, Iran University of Science and Technology, Tehran, Iran

ABSTRACT

The measurement of the minimum miscibility pressure (MMP) is one of the most important steps in the project design of miscible gas injection for which several experimental and modeling methods have been proposed. On the other hand, the standard procedure for compositional studies of miscible gas injection process is the regression of EOS to the conventional PVT tests. Moreover, this procedure does not necessarily result in an accurate calculation of the MMP. In this study, an effective procedure is presented using both conventional PVT and slim tube data in the regression to provide appropriate EOS parameters for field studies including miscible gas injection. In the first step, the EOS parameters were subjected to regression to the conventional PVT data. In addition, these parameters were then used as inputs for simultaneous regression to the conventional PVT and MMP data. MMP is modeled through the automated execution of a series of compositional simulation of slim tube. Moreover, the regression uses a stochastic optimization for minimizing an objective function (regression) have been coupled with two separate core calculations, (1) equilibrium calculations of the conventional tests and (2) compositional simulation of the slim tube. For evaluation, a number of real reservoir fluids from field data are used from reliable datasets in the literature. Finally, the promising results demonstrated that this procedure is capable to provide EOS parameters for accurate predictions in the miscible gas injection processes.

Keywords: Reservoir Fluids, Minimum Miscibility Pressure, Compositional Simulation, Regression, Slim Tube.

INTRODUCTION

Miscible and immiscible gas injection are two main categories of gas injection processes. Miscible gas injection has several advantages over immiscible gas injection. The advantages include (1) reduction in oil-gas surface tension, (2) reduction in oil viscosity, (3) oil mobility increment, (4) reduction in capillary pressure, (5) oil swelling, and so on. However, knowing its concepts and designing parameters have been subjected to considerable changes and as a result, currently, more factors are required to be considered in conducting an efficient and successful operation. The pressure under which miscibility occurs through finite contacts between gas and oil is known as minimum miscibility pressure (MMP). Moreover, MMP is the minimum pressure

***Corresponding author**
Mehdi Assareh
Email: assarehm@iust.ac.ir
Tel: +98 21 7724 3025
Fax: +98 21 7724 0495

Article history
Received: August 08, 2018
Received in revised form: October 26, 2018
Accepted: November 26, 2018
Available online: May 21, 2019
DOI: 10.22078/jpst.2018.3270.1537

at which gas and oil become miscible in any given proportion. By increasing pressure beyond MMP and within a dispersion free system, the recovery factor does not change significantly; therefore, MMP is the optimum pressure for injection. This highlights and emphasizes the significance of a precise determination of the MMP [1].

EXPERIMENTAL PROCEDURE

There are different experiments for the MMP measurement; for example, vanishing interfacial tension [2], slim tube [3, 4], high pressure visual sapphire cell [5], falling drop technique [6], pressure-composition diagram [7], mixing-cell experiments [8-10], rising bubble apparatus [11], and vapor density [12]. Also, MMP values were investigated by Abedini et al [13] by analyzing swelling factor curves. In addition, a number of recently developed experimental techniques have been used for MMP measurements [14]. In the work of Liu et al [15] and Czarnota et al [16], new experimental approaches have been proposed. Moreover, some experimental methods for the measurement of MMP value such as rising bubble apparatus, PVT cell, pendant drop, and IFT vanishing usually result in the overestimation of the MMP. According to Zick [17], these single cell methods cannot show the complexity of vaporizing-condensing mechanisms for miscibility development. The error in these methods also increases with fluid complexity growth [18]. In addition, miscibility is a dynamic process, happening through numerous contacts between the initial fluid and enriched injected gas (condensing) or/and altered reservoir fluid, and lean injected gas (vaporizing). Therefore, the experimental techniques in which multiple contacts are achieved for miscibility are more fitted to miscible gas injection in reservoirs. Moreover, the slim tube, as a standard experimental approach, is a helical tube, filled with sand particles. Initially, it is saturated by reservoir fluid at a pressure which is greater than the bubble point pressure of the reservoir oil. The gases are injected from a gas accumulator at different pressure steps, and recovered oil is collected after 1.2 pore volume for each step. Also, the recovery factor (RF) curve for each pressure step shows MMP as an intersection point. Finally, the MMP (minimum miscibility pressure) measured from slim-tube is the most acceptable result. This is due to the fact that the reservoir fluid is used to determine MMP.

MMP Modeling Approaches

As a general classification, one can divide MMP modeling approaches into two categories: (1) data-driven models and (2) EOS based models. In the first category, a number of MMP correlations have been proposed based on the experimental data for a limited range of the reservoir oil and gas properties. Moreover, empirical correlations are always attractive for fast estimations, and they can be useful in cases where complete experimental data are not available. Recently, a number of powerful models have been published in the literature to estimate MMP using artificial intelligence techniques, for example, the work of Zhong and Carr [19], Ahmadi et al [20].

In the second category, MMP is modeled according to an EOS for the tests including multiple contacts. These methods can be categorized into two main groups: analytical and numerical methods. The first set of analytical methods, are for example those proposed by Johns and Orr [21] and developed by Wang and Orr [22]. These methods actually

involve a graphical tie line method extension to real systems [23]. In the analytical method, gas and oil are considered in two separate mixing cells, then they get mixed and flashed. The liquid and the gas obtained are then placed in the new cells. Successive cells mixing is maintained until the key tie lines are determined which happens when tie line length is the same for three successive cells. When the length of one of these key tie lines reduces to zero, the miscibility is achieved. The main difference in the approaches is to the procedure of selecting the next step pressure and the shock assumption. [24-30]. There are many recent publications in this area, however, there is a limited application for real reservoir fluids. Moreover, calculations using numerical methods (those fit multiple contacts) are also based on EOS, and their accuracy depends upon EOS capability in modeling fluid phase behavior. In these methods, a series of mixing cells is defined in one dimension as a medium for miscibility development. Also, a multiple mixing cells method has been proposed by Metcalfe et al [31] for the first time to perform MMP calculations. In their method, a series of cells containing initial oil is considered. Also, gas is injected into the first cell in a determined proportion. The fluid is then flashed, and excess fluid is transferred to the next cell.

Researchers in this area are not unanimous on the type of transfer function. Injection is continued until the quantity of injected gas reaches 1.2 pore volume. Discharged fluid from the last cell is flashed under standard conditions, and gathered liquid volume is used to calculate the recovery factor (RF) [31-33]. One of the most practical revisions of multiple mixing methods, is the method of Jaubert et al [33]. They considered an exponential trend for the recovery factor versus pressure. By fitting an exponential curve to three recovery factor points, the pressure, corresponding to 97% recovery factor, is considered as MMP. It is shown by Jaubert et al [33] that plotting recovery factor versus the inverse value of the number of cells' square root (1/√N) will form a straight line. Moreover, the recovery factor extrapolation to zero (infinite cell number) ensures the MMP value to be independent of the limited number of cells [33]. A 1D compositional reservoir model with an injection and a production well, representing a slim-tube, is one of the best and easiest methods in this regard [23]. A 1D simulator has been developed by Yan, et al [34] and it has been mentioned by them that the methods resemblance to slim-tube as its best advantage. They have also mentioned that more details could be included in slim-tube simulators such as pressure solution, capillary effect, dispersion effect, and realistic relative permeability models. This means that the MMP modeling through this approach and including all effective mechanisms requires a series of the simulation run with a compositional simulator engine. Such methods require several runs and visual plots to obtain MMP.

MMP Regression

The common industrial practice for the reservoir fluid modeling and compositional simulation of the gas injection process, is to use an EOS and tune its uncertain parameters through regression to the conventional PVT experiments (saturation pressure calculation, constant composition expansion, differential liberation, separator test, etc.). The measured MMP is not used commonly to improve the regressed equation of state. Moreover, the importance of tuning EOS to MMP has been indicated by Egwuenu et al [35].

They used an analytical approach to calculate MMP and after tuning EOS with conventional PVT tests has been used by Egwuenu et al. Afterward, experimental MMP to tune EOS parameters has been used by them.

It is stated by them that tuning of EOS parameters with a swelling test alone may result in a poor MMP match; however, tuning to both conventional PVT experiments (here, swelling data) and MMP can be fitted well for both types of experiments. In addition, the idea of tuning the fluid model with MMP (through EOS based modeling considering multiple contacts) value was first proposed by Negahban and Kremesec [36] where they tuned C_{+7} properties to match MMP results using a vaporizing MMP calculation method. Also, a model was used to calculate MMP by Jaubert et al [37]. It was shown by Jaubert et al that by matching swelling test data and multiple contact experiments using critical pressure (Pc) and critical temperature (Tc) of heavier fractions as matching parameters, MMP can be matched within an acceptable deviation of 5%. The Work of This Study The main focus of this work is on presentation and evaluation of an automated and accurate procedure to improve EOS parameters already regressed to conventional PVT experiments for MMP modeling using a compositional simulation of slim tube. There are limited researches about MMP regression, but none of them, used a compositional simulator, which is a representative of the real slim-tube. To match MMP, an automated method is required to calculate it without a manual work around (since the compositional simulation engines are separated from the conventional PVT study package, an execution automation is required). In this work, a compositional simulator is selected for MMP calculation.

With this core calculation of MMP, the deviation from the experimental data is included in an objective function. In addition, bubble point pressure and saturated liquid density modeling are programmed to calculate the deviation from experimental data. The calculated deviations are also included in the objective function for the final regression. This generates an EOS set of parameters which takes advantage of PVT tests plus slim-tube test for miscible gas injection. This work highlights and emphasize the following items:

- Automatic MMP detection from a series of compositional simulation of a slim tube,
- Use of real petroleum samples to validate MMP modeling and regression workflows, and
- Simultaneous regression of MMP and conventional PVT data.

The slim-tube simulation consists of a series of 1D model of similar simulation cells. These cells are fully saturated with oil and are under the same pressure. An injection well and a production well are considered in the first cell and the last cell respectively. The injection is simulated at a constant rate of one tenth of pore volume (PV) per hour and it is continued for 12 hours; therefore, at the end of simulation, 1.2 PV is already injected into the 1D (one dimensional) reservoir model. Production well bottom-hole pressure is the same as cells pressure; hence, there is no considerable pressure gradient in the system. The recovery factor should be recorded for each pressure and by increasing pressure, the recovery factor trend versus pressure is obtained.

Figure 1 shows the grid model schematically. Different criteria have been proposed in the literature to find MMP from the calculated recovery data versus test pressure.

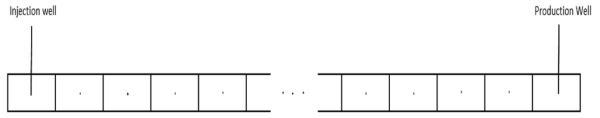

Figure 1: Slim-tube discretized model in the compositional simulation data file, the injection well is controlled by constant voidage rate and the production well is controlled by constant bottom-hole pressure.

In addition, (1) reaching a certain amount of recoveries such as 90, 95, and 97 % of the maximum amount of recovery factor versus pressure, intersection of low recovery line and high recovery line, (2) reaching certain amount of GOR at a certain recovery factor are all examples of criteria used in the literature [29, 38, 39]. In this work, a research code is programmed in C# to implement the proposed procedure. After providing a regular EOS tuning to conventional PVT data, the required data are extracted. The compositional simulator executable file is run automatically with slim tube data file using "Process" objects from the System's Diagnostic Library in C#.

The data file is then inputted automatically for the different pressures (written to the data file) altered from a high pressure value up to bubble point pressure. Moreover, pressure should be assigned in all the cells as well as in the production well. The reservoir simulation data file usually contains, several sections, for example, model dimension, numerical run information, grid geometry, and simulation blocks static properties, rock-fluid saturation function, component critical properties, and EOS required information (which is filled with the output of EOS parameter sets after conventional test regression), initialization, and production/ injection schedule. During the calculation of MMP, only, the two last sections are required to be updated with such pressure to calculate the corresponding recovery factor.

The high pressure is supposed to be the first contact miscibility pressure which can be obtained roughly from the conventional PVT software. If experimental MMP is available, this pressure can be a point with a reasonable distance from it. The pressure step length can be altered regarding the different regions of the recovery factor curve. As an example, in this work, pressure steps are reduced in low recovery region due to steep changes in this factor below the MMP. An 8 [atm] pressure step length has been considered for the high recovery region. In the next step, this pressure was lowered to 2 [atm] immediately after recording the recovery factor less than 90%. After saving various recovery factors versus different pressures, the calculations should be repeated for several cells. To eliminate the numerical dispersion effect, a linear dependency of recovery factor to 1/N is considered, and the recovery factor of an infinite number of cells is determined through finding recovery factor versus 1/N intercept. In addition, the pressure derivative and curvature of infinite recovery factor are calculated and the maximum pressure curvature is determined. This point divides the points into high-recovery and low-recovery regions.

The smoothest point is then located in the high-recovery region by locating the minimum value of the second derivative. The points with small slope difference (less than 0.01) from this point, are considered as the high recovery points. In the low-recovery region, due to various behavior and curvature for different fluids, determining a

similar restriction is not feasible. It was observed that all points with 70 to 84% recovery were on the low recovery line in all of the graphs. Therefore, in this study, the pressure points with 70 to 84% recovery are considered as low-recovery points. By limiting the calculations to the recovery factor of 70%, the computational load is reduced considerably.

Two lines are then fitted to low and high recovery points by the least square method. The intersection of these two lines is considered as MMP. The automatic MMP calculation procedure is shown in Figure 2.

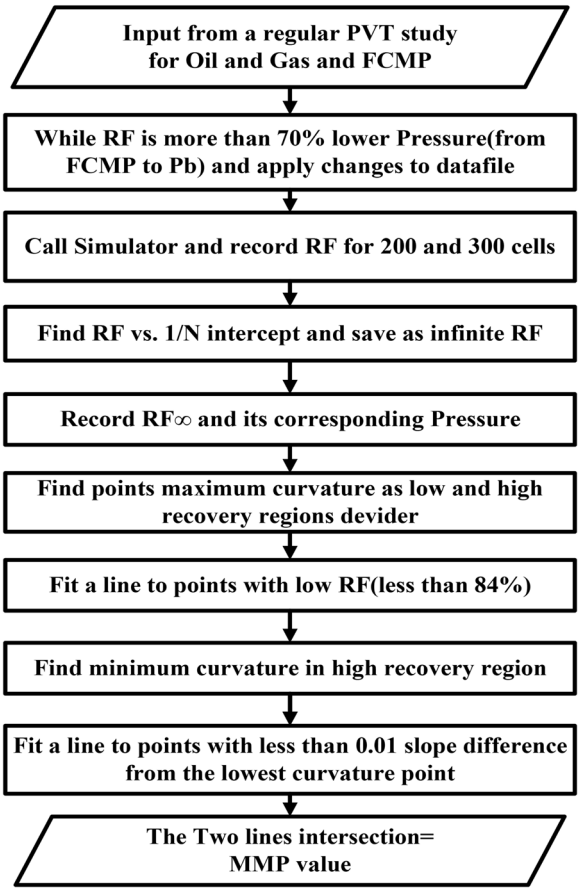

Figure 2: Automatic MMP calculation procedure, using a compositional simulation engine.

One of the main advantages of MMP calculation using slim tube compositional simulation is its easy programming implementation relative to the method of characteristics or mixing cell techniques. Because, it is just a series of compositional simulation runs through automated calling compositional simulator engines from the commands. Therefore, the reservoir engineers working on the field study of the gas injection process can directly incorporate the miscible injection test into their reservoir fluid study model without extra programming for the MMP modeling. The compositional simulation engines solve the linearized discretized mole balance (for all hydrocarbon components) equations in simulation grid blocks simultaneously, in each simulation time-step. In addition, the equivalence of the components fugacity liquid and vapor phase must be observed for each simulation cell in a time-step. In another word, EOS has two main roles in compositional simulation: (1) the first role is the calculation of the physical properties (like viscosity and density) of oil and gas in a slim tube and the oil-gas surface tension. (2) The second role is the calculation of fugacity to solve the oil-gas fugacity equivalence equations for all hydrocarbon components in each simulation cell in a time-step.

Model Regression

As mentioned before, MMP calculation using compositional simulator is an EOS based method and its accuracy depends highly on EOS capability to predict fluid behavior. An EOS model, which is regressed to the bubble point and constant composition expansion (CCE) / differential liberation (DL) tests, does not necessarily provide accurate MMP. Even if the real slim tube results are available for a fluid, the fluid model cannot be improved to fit the experimental MMP by commercial software using compositional simulation of slim tube. Also, a fluid model which is not capable of predicting MMP with little deviation cannot be used for accurate simulation of an oil field with gas injection.

Moreover, a precise fluid model is necessary to determine the optimum enrichment in order to reach miscibility around the reservoir pressure. In order to have the best EOS parameters which reproduce the experimental MMP and conventional tests, a procedure is proposed to regress the fluid model. In this procedure, saturated liquid density, bubble point, and MMP calculations are coupled into an optimization algorithm which is then employed to minimize the bubble point pressure, saturated liquid density, and MMP deviations from the experimental data simultaneously.

In other words, an objective function (Equation 1) is constructed from bubble point pressure, saturated liquid, and MMP deviations with weighing factors:

$$Objective\,Function = weight_{Pb} \times \left| \frac{\left(Pb_{real} - Pb_{calc}\right)}{Pb_{real}} \right| + weight_{liq\,dense} \times \left| \frac{\left(liq\,dense_{real} - liq\,dense_{calc}\right)}{liq\,dense_{real}} \right| + weight_{MMP} \times \left| \frac{\left(MMP_{real} - MMP_{calc}\right)}{MMP_{real}} \right| \quad (1)$$

This is a common objective function of commercial PVT software, which is also implemented in our code. It shows a weighted sum of relative deviations from conventional and miscible experiments. In this study, simulated annealing (SA) was used as the optimization algorithm. Simulated Annealing is a powerful stochastic optimization algorithm. SA algorithm mimics the process undergone by misplaced atoms in a heated metal and then slowly cooled in order to reach the maximum crystal size and reduce its defects to find the global optimum point. The advantage of simulated annealing over other gradient based methods is that it avoids getting caught at local optimums to find the global optimum point. The probability check in this algorithm has ensured this aim. The optimization begins with an initial value. The function value is then calculated, and its value and its corresponding altering parameters are saved as the minimum and accepted values. After defining an upper and a lower limit for each parameter, a neighborhood search is performed in the point's vicinity and the function is calculated. If the function value is less than the currently accepted function value, the accepted values are replaced with new values and if they are also less than minimum function, the minimum parameters are replaced as well. However, the accepted function values are replaced with the new values for the higher function for a better result and escaping from local minima. This step is done in the probability check stage of the flowchart. These steps are continued for a determined number of trials. The regression (optimization) code was written in C# language. Bubble point and liquid density calculations are also programmed in C#. In addition, automation of MMP finding by compositional simulator was written in C#. The compositional simulator was ECLIPSE (E300). To describe a general view of the regression approach, a schematic diagram of the required steps is presented in Figure 3.

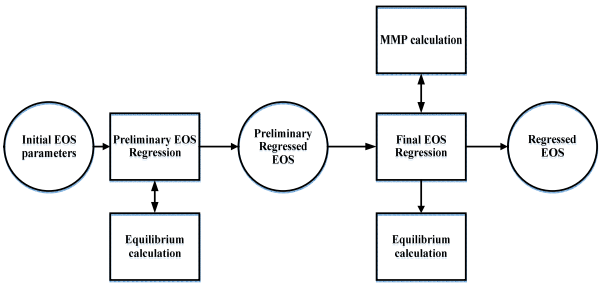

Figure 3: General steps of the proposed work flow, the EOS section of the simulation data file for MMP calculation is continuously updated within the final regression.

An initial fluid model is constructed using a regular PVT study. The correlations for the heavy fractions, critical and thermos-physical properties are summarized in Table 1.

Table 1: Correlations used to calculate initial properties of EOS before preliminary regression.

Parameter	Correlation
Critical Properties	Kesler and Lee [43]
Acentric Factor	Kesler and Lee [43]
Binary Interaction Coefficients	Whitson [44]
Viscosity	Lohrenz, et al. [45]
Independent Volume Shift	Jhaveri and Youngren [46]

Two-parameter cubic EOSs, for example Peng-Robinson [40], gives inaccurate liquid density estimations. Therefore, three-parameter cubic EOS is used. In this work, the three-parameter Peng-Robinson EOS with correction term (improved dependency to the acentric factor of heavy hydrocarbon species) is used in the calculations. The conventional PVT tests are simulated using the equivalence of fugacity and saturation conditions with the aid of EOS. The model is then regressed based on the conventional tests, by changing the critical values for two of the heaviest components (critical pressure, critical temperature and acentric factor) with estimated uncertainty (30% for the heaviest component (C_{+20}) and 10% for the other one) as well as their volume shift and binary interaction coefficients with methane.

As it is shown in Figure 3, MMP and target function calculation is performed for the preliminary regressed model. The preliminary regressed model is then introduced to the SA algorithm.

This is followed by an optimization implemented in two steps. In the first step, critical values (critical pressure, critical temperature and acentric factor) of the two heaviest components are altered based on optimizing procedure (limited to 30% uncertainty for the heaviest component and 10% uncertainty for the second heaviest from their initial value). After saving the minimum target function and regarding altered parameters, the first-step optimized model enters the second level of optimization. In the second level, the heaviest component binary interaction coefficients with methane, ethane, and the two heaviest components' volume shifts are considered as optimization parameters. The volume shifts, while alternation, is limited to zero and 150% of their initial values. The changes are then implemented in PVT data that is an input file for the compositional simulator. Meanwhile, the minimum function is recorded in each step. The parameters of the final minimum function make the optimum fluid model for predicting MMP and bubble point simultaneously.

Real Oil and Gas Samples

A number of real reservoir fluids from Jaubert et al [41] were used to evaluate the proposed procedure. The studied samples in this study are presented in Tables 2 and 3.

The samples' components were grouped based on the heaviest component in the gas sample. The mixing rules for the calculation of the groups' critical properties were EOS-based mixing rules. There are numerous ways to mix the properties, all giving different results. In addition, mixing rules are applied for calculating the properties of a pseudo-component from its component critical and thermo-physical properties [42]. It is better than, the non-hydrocarbon components and the components with high mole fraction (like methane and plus fractions) are not included in

the grouping process [42]. To ensure the minimum effect of grouping on the phase plot, all of the gas components heavier than C_6 were grouped with each other.

Also, the heavy components in the oil phase were lumped excluding C_{+20}. The association of C_{+20} with a group can change the phase plot considerably, since it is a key component with a relatively high mole fraction and considerably different critical properties. The parameters of pseudo-components were calculated using EOS-based mixing rules using the oil phase composition. The pseudo-components' molecular weight and specific gravity are provided in Table 4.

Table 2: Sample#1 to Sample#4 oil composition.

Oil # 1		Oil # 2		Oil # 3		Oil # 4	
Component	**Mole Percent**	**Component**	**Mole Percent**	**Component**	**Mole Percent**	**Component**	**Mole Percent**
N_2	0.200	N_2	0.450	N_2	0.350	N_2	0.450
H_2S	0.000	H_2S	0.000	H_2S	0.000	H_2S	0.383
CO_2	1.340	CO_2	1.640	CO_2	3.140	CO_2	2.070
C_1	23.640	C_1	45.850	C_1	54.260	C_1	26.576
C_2	8.560	C_2	7.150	C_2	8.570	C_2	7.894
C_3	6.680	C_3	6.740	C_3	5.720	C_3	6.730
C_4	5.300	C_4	3.950	C_4	3.210	C_4	5.384
C_5	4.450	C_5	2.680	C_5	1.950	C_5	4.442
C_6-C_9	16.760	C_6-C_8	10.570	C_6-C_9	9.250	C_6-C_8	11.795
C_{10}-C_{19}	21.040	C_9-C_{19}	14.790	C_{10}-C_{19}	9.470	C_9-C_{19}	21.314
C_{+20}	12.030	C_{+20}	6.180	C_{+20}	4.080	C_{+20}	12.962

Table 3: Sample#5 to Sample#8 oil composition.

Oil # 5		Oil # 6		Oil # 7		Oil # 8	
Component	**Mole Percent**	**Component**	**Mole Percent**	**Component**	**Mole Percent**	**Component**	**Mole Percent**
N_2	0.000	N_2	0.000	N_2	0.083	N_2	0.400
H_2S	0.000	H_2S	0.000	H_2S	0.000	H_2S	0.355
CO_2	0.774	CO_2	2.130	CO_2	1.824	CO_2	2.548
C_1	36.203	C_1	31.280	C_1	32.165	C_1	47.244
C_2	9.736	C_2	7.510	C_2	7.627	C_2	6.937
C_3	6.745	C_3	6.930	C_3	7.221	C_3	4.805
C_4	4.959	C_4	6.260	C_4	6.507	C_4	4.253
C_5	3.894	C_5	4.740	C_5	5.018	C_5	3.405
C_6-C_8	10.404	C_6-C_{12}	25.520	C_6-C_{12}	24.162	C_6-C_8	8.797
C_9-C_{19}	19.138	C_{13}-C_{19}	9.300	C_{13}-C_{19}	8.691	C_9-C_{19}	15.251
C_{+20}	8.147	C_{+20}	6.330	C_{+20}	6.702	C_{+20}	6.005

Table 4: Pseudo components Specific gravity and molecular weight for each sample after characterization.

Oil # 1			Oil # 2			Oil # 3			Oil # 4		
component	Specific gravity	MW	component	Specific gravity	MW	component	Specific gravity	MW	component	Specific gravity	MW
C_6-C_9	0.718	102.68	C_6-C_8	0.725	96.24	C_6-C_9	0.733	103.28	C_6-C_8	0.722	96.49
C_{10}-C_{19}	0.815	185.51	C_9-C_{19}	0.812	171.71	C_{10}-C_{19}	0.813	183.21	C_9-C_{19}	0.824	178.41
C_{+20}	0.949	530.00	C_{+20}	0.825	474.00	C_{+20}	0.905	418.00	C_{+20}	0.956	450.00
Oil # 5			**Oil # 6**			**Oil # 7**			**Oil # 8**		
component	Specific gravity	MW	component	Specific gravity	MW	component	Specific gravity	MW	component	Specific gravity	MW
C_6-C_8	0.713	95.62	C_6-C_{12}	0.745	115.71	C_6-C_{12}	0.740	116.62	C_6-C_8	0.712	94.06
C_9-C_{19}	0.805	170.04	C_{13}-C_{19}	0.831	210.01	C_{13}-C_{19}	0.827	214.51	C_9-C_{19}	0.804	172.03
C_{+20}	0.938	442.00	C_{+20}	0.915	455.00	C_{20+}	0.915	455.00	C_{+20}	0.917	434.00

Using this table, and with the correlations of Table 1, the results of this work are reproducible by readers. The mean bubble point pressure over the samples is 19.56 [MPa], and it is in the range of 11.77 to 32.02 [MPa]. The mean saturated liquid density over the samples is 647.14 [kg/m^3], and it is in the range of 545.55 [kg/m^3] to 741.8 [kg/m^3]. The mean minimum miscibility pressure over the samples is 31.43 [MPa], and it is in the range of 23.50 to 37.90 [MPa]. The gas samples' composition from Jaubert et al [41] are tabulated in Tables 5 and 6.

Table 5: Sample#1 to Sample#4 gas composition.

Gas # 1		Gas # 2		Gas # 3		Gas # 4	
Component	Mole Percent	Component	Mole Percent	Component	Mole Percent	Component	Mole Percent
N_2	0.480	N_2	0.490	N_2	0.410	N_2	0.000
H_2S	0.000	H_2S	0.000	H_2S	0.000	H_2S	0.000
CO_2	4.960	CO_2	1.820	CO_2	1.650	CO_2	0.000
C_1	58.050	C_1	81.390	C_1	81.710	C_1	88.000
C_2	17.090	C_2	9.150	C_2	9.160	C_2	7.000
C_3	11.970	C_3	4.670	C_3	4.540	C_3	3.000
C_4	4.960	C_4	1.740	C_4	1.690	C_4	1.000
C_5	1.660	C_5	0.460	C_5	0.450	C_5	1.000
C_6-C_9	0.830	C_6-C_8	0.280	C_6-C_9	0.390	C_6-C_8	0.000

Table 6: Sample#5 to Sample#8 gas composition.

Gas # 5		Gas # 6		Gas # 7		Gas # 8	
Component	**Mole Percent**	**Component**	**Mole Percent**	**Component**	**Mole Percent**	**Component**	**Mole Percent**
N_2	0.420	N_2	0.000	N_2	0.000	N_2	0.220
H_2S	0.250	H_2S	0.000	H_2S	0.000	H_2S	2.720
CO_2	2.850	CO_2	4.350	CO_2	4.350	CO_2	4.430
C_1	75.550	C_1	81.140	C_1	81.140	C_1	66.100
C_2	14.340	C_2	10.310	C_2	10.310	C_2	6.410
C_3	5.520	C_3	3.320	C_3	3.320	C_3	12.040
C_4	0.960	C_4	0.880	C_4	0.880	C_4	7.430
C_5	0.100	C_5	0.000	C_5	0.000	C_5	0.470
C_6-C_8	0.010	C_6-C_{12}	0.000	C_6-C_{12}	0.000	C_6-C_8	0.180

From the tables, it can be understood that, two gas samples contain hydrogen sulfide. The samples 4, 6, and 7 do not contain nitrogen, and only sample 4 does not contain carbon dioxide (which leads to a high experimental MMP). In a case, that the reservoir fluid mixture is not reported up to C_{+20}, it is recommended to prepare the reservoir fluid sample through splitting/grouping.

RESULTS AND DISCUSSION

The initial parameters of EOS model are regressed (in the preliminary regression stage) to the conventional experiments by changing the two heaviest components critical values (up to 30% for the heaviest, C_{+20}, and 10% for the next heavy component), their volume shifts (for the two heaviest fractions) and C_{+20} binary interaction coefficients with methane and ethane. The other hydrocarbon-hydrocarbon binary interaction coefficients are set to zero. The binary interaction coefficients among non-hydrocarbon components are kept at their initial values. The preliminary regression results have indicated that resetting the most of the hydrocarbon-hydrocarbon binary interaction coefficients to zero (excluding methane with the two heaviest hydrocarbons) leads to a better MMP prediction. In addition, setting most of these coefficients to zero simplifies the model and by reducing the number of uncertain parameters, it makes the model optimization procedure easier.

Before preliminary regression, the set of parameters are named “initial” in this manuscript. It means those parameters have been calculated from Table 1. After the preliminary regression, the suitable EOS parameters to simulate conventional PVT tests are determined. These parameters are referred to as “Matched” in this work. However, according to the explanations in the introduction section, it is not accurate to use this set of parameters for field study of the gas injection process, since regression to conventional test does not guarantee a good estimation of the MMP.

Therefore, the prepared workflow for automated detection of MMP is used to calculate MMP from compositional simulation of the slim tube with “Matched” set of EOS parameters for the reservoir fluid. This set of parameters serve as the initial guess for the secondary stage of regression, wherein parameters are further subjected to optimization to match bubble point pressure and saturated liquid density (from the conventional tests), and

MMP (for the gas injection test). In this regression, the core calculation of MMP using the engine of a compositional simulator, is executed several times along with conventional equilibrium calculation to provide the deviation objective function (which should be minimized). The set of parameters after this final regression is referred to as "Optimized" in this work. This sequential approach of regression (at first regression to conventional tests and then regression to both conventional and gas injection tests) helps optimize the higher priority conventional tests (from the usage point of view) and then fine tune the optimization variables (or change the variables a little) to adopt MMP. Moreover, our simultaneous optimization test was not successful. In a simultaneous regression test, although the deviation of MMP from the experiments becomes smaller, the deviations in the conventional test become larger.

The properties of the pseudo-components in each step of the regression procedure ("Initial", "Matched" and "Optimized") are shown in Tables 7 and 8.

Table 7: Sample#1 to Sample#4 pseudo components' properties (critical pressure, critical temperature, acentric factor and dimensionless volume shift), before preliminary regression, after preliminary regression and after final regression.

	Phase	Component	P_c (bar)	T_c (K)	ω	S shift
Sample #1	Initial	C_{10}-C_{19}	18.33	684.94	0.6088	0.1405
		C_{+20}	5.47	1005.40	1.4921	0.5277
	Matched	C_{10}-C_{19}	18.89	732.88	0.6647	0.1400
		C_{+20}	6.77	1290.90	1.6292	0.5523
	Optimized	C_{10}-C_{19}	19.23	732.53	0.6128	0.1405
		C_{+20}	6.88	1069.76	1.8485	0.5277
Sample #2	Initial	C_9-C_{19}	20.09	666.43	0.5547	0.1035
		C_{+20}	4.68	890.22	1.4352	0.5637
	Matched	C_9-C_{19}	19.81	697.50	0.5269	0.1059
		C_{+20}	5.54	1116.50	1.6361	0.3236
	Optimized	C_9-C_{19}	21.52	599.79	0.4992	0.1035
		C_{+20}	5.33	1123.95	1.8021	0.5637
Sample #3	Initial	C_{10}-C_{19}	18.45	683.47	0.6054	0.1421
		C_{+20}	7.52	915.97	1.2728	0.4458
	Matched	C_{10}-C_{19}	19.77	688.69	0.5569	0.1149
		C_{+20}	9.67	1051.04	1.0040	0.2219
	Optimized	C_{10}-C_{19}	16.61	664.20	0.6167	0.1421
		C_{+20}	7.63	1042.04	1.3249	0.4521
Sample #4	Initial	C_9-C_{19}	19.90	682.23	0.5740	0.1084
		C_{+20}	7.55	968.63	1.3155	0.4611
	Matched	C_9-C_{19}	21.35	672.23	0.5311	0.1059
		C_{+20}	9.72	1089.00	1.0998	0.3236
	Optimized	C_9-C_{19}	20.60	614.01	0.6100	0.1108
		C_{+20}	9.30	1259.22	1.0300	0.4190

Table 8: Sample#5 to Sample#8 pseudo components' properties (critical pressure, critical temperature, acentric factor and dimensionless volume shift), before preliminary regression, after preliminary regression and after final regression.

	Phase	Component	P_c(bar)	T_c(K)	ω	S shift
Sample #5	Initial	C_9-C_{19}	20.04	661.08	0.5502	0.1010
		C_{+20}	7.43	951.61	1.3096	0.4600
	Matched	C_9-C_{19}	19.04	661.08	0.5502	0.1010
		C_{+20}	8.44	921.94	1.3096	0.4301
	Optimized	C_9-C_{19}	19.17	624.39	0.5841	0.1012
		C_{+20}	8.24	1087.84	1.2354	0.4651
Sample #6	Initial	C_{13}-C_{19}	16.87	721.50	0.6820	0.1571
		C_{+20}	6.64	942.70	1.3540	0.4875
	Matched	C_{13}-C_{19}	18.56	751.79	0.6480	0.1571
		C_{+20}	8.76	1131.20	1.3990	0.4875
	Optimized	C_{13}-C_{19}	18.39	753.45	0.6290	0.2602
		C_{20+}	8.26	1192.65	1.1990	0.5072
Sample #7	Initial	C_{13}-C_{19}	16.24	722.44	0.6992	0.1680
		C_{+20}	6.64	942.70	1.3542	0.4875
	Matched	C_{13}-C_{19}	16.24	722.44	0.6992	0.1680
		C_{+20}	8.63	1011.29	1.3542	0.3696
	Optimized	C_{13}-C_{19}	15.24	650.20	0.7414	0.1706
		C_{+20}	8.27	957.27	1.6401	0.4527
Sample #8	Initial	C_9-C_{19}	19.76	663.01	0.5573	0.1046
		C_{+20}	7.27	933.08	1.3040	0.4602
	Matched	C_9-C_{19}	19.45	704.72	0.5016	0.1046
		C_{+20}	8.56	993.79	1.0588	0.4112
	Optimized	C_9-C_{19}	20.43	713.14	0.5825	0.1512
		C_{+20}	6.85	1042.01	1.3502	0.4508

In short, "Initial" means the basic EOS calculation without regression. Therefore, the critical properties are calculated using the mentioned correlations (as in Table 1); "Matched" means the EOS parameters subjected to the preliminary regression to the conventional PVT experiments; "Optimized" means the EOS parameters in the final regression step. The parameters of the preliminary regressed model are presented in the matched phase row, where those in optimized row, are from SA algorithm output in the final regression. According to these two tables, the volume shifts of the two last pseudo-components after final regression are generally close to the initial values, however volume shifts before and after final regression are considerably different. For other parameters like critical pressure, critical temperature, and acentric factor, there is no such general trend over the samples. As an example, the step function value, accepted function value, and minimum function value alternation, for the regression with the simulated annealing, for one of the samples (sample 4) in each iteration is shown in Figure 4.

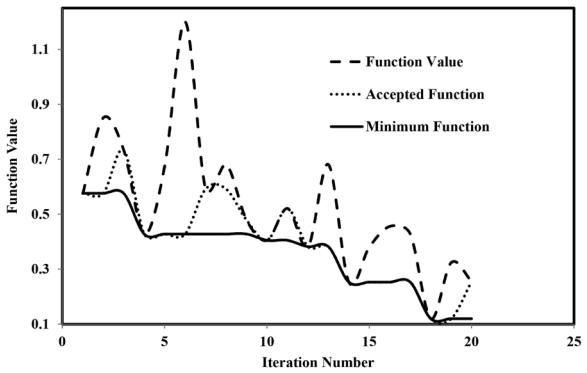

Figure 4: Objective function, Accepted objective function and Minimum function value in each iteration of optimization for a sample using simulated annealing.

The optimizations were performed in 20 iterations batches. If the results were not promising, the algorithm output model parameters were presented to it once again. Considering the importance of the bubble point pressure, the weight assigned to it, in the optimization process, was set to 6. In addition, for MMP and saturated liquid density, weights were set to 3 and 3 (the weights were high enough to show deviations) respectively. The non-zero hydrocarbon-hydrocarbon binary interaction coefficients are also presented in Table 9.

Table 9: Binary interaction coefficients (between heaviest component-methane, and heaviest component-ethane), before preliminary regression, after preliminary regression and after final regression.

	initial values		Matched values		Optimized values	
C_{+20} binary	C_1	C_2	C_1	C_2	C_1	C_2
Sample #1	0.0649	0.01	0.0349	0.02	0.0649	0.01
Sample #2	0.0475	0.01	0.0951	0.02	0.0475	0.01
Sample #3	0.0587	0.01	0.0510	0.0014	0.0588	0.01201
Sample #4	0.0658	0.01	0.0644	0.02	0.0509	0.009
Sample #5	0.0633	0.01	0.1300	0.024	0.0657	0.013
Sample #6	0.0600	0.01	0.0047	0.0038	0.0696	0.011
Sample #7	0.0600	0.01	0.0600	0.01	0.0695	0.0148
Sample #8	0.0604	0.01	0.0900	0.02	0.0390	0.008

The range of alteration shows increments from zero to at most 150%. It is concluded from the calculations that although the binary interaction coefficients affect MMP, they can change bubble point calculations simultaneously. The results in Table 10 are MMP and bubble point calculations in the "Initial", "Matched" and "Optimized" phases. Also, "matched" row values demonstrate how erroneous a preliminary matched model can be for MMP calculation.

Moreover, the "Optimized" row results indicate the progress made from the optimization algorithm and the method's important part in reducing the MMP calculations deviation at the same time with matching bubble point pressure and saturated liquid density. For comparison, the average absolute deviation percent (%AAD) is calculated using the following equation (Equation 2):

$$AAD\% = \frac{1}{nsample} \sum_{isample} \left| \frac{\emptyset^{exp} - \emptyset^{calc}}{\emptyset^{exp}} \right|_{isample} \quad (2)$$

where nsample is 8, and isample is sample counter, Ψ is the target value for which the deviation is calculated (it can be bubble point pressure, saturated liquid density, and minimum miscibility pressure). Table 10 can provide a number of concluding remarks. In In Table 10, AAD% of miscibility pressure is 13.3% with "initial" parameters set, 12.5% with "matched" parameters set and 0.3% with "optimized" set of parameters. This shows that, even though, the average relative deviation has been reduced from 13.3% to 12.5% during the conventional tests regression step, the deviation is still considerable. Besides, the final stage of regression (regression to MMP, bubble point pressure and saturated liquid density) was very helpful to have a more general set of parameters for EOS. In Table 10, AAD% of

Table 10: Initial (before preliminary regression to conventional tests), Matched (after preliminary regression to conventional tests) and Optimized (after regression to both conventional and MMP test) values for MMP, bubble point pressure and saturated liquid density for each sample including corresponding sample experimental data.

	Sample #1	Sample #2	Sample #3	Sample #4	Sample #5	Sample #6	Sample #7	Sample #8
Initial MMP (MPa)	23.18	31.54	38.35	44.53	34.6	32.28	33.29	22.94
Matched MMP (MPa)	27.78	39.44	40.83	43.62	34.11	34.58	31.64	27.75
Optimized MMP (MPa)	23.47	37.5	38.04	36.68	31.5	29.63	26.23	28.56
Experimental MMP (MPa)	23.5	37.6	37.9	36.6	31.3	29.6	26.25	28.69
Initial Pb (MPa)	8.45	15.91	27	12.81	15.43	12.24	12.9	22.05
Matched Pb (MPa)	11.77	25.56	32.02	14.58	17.29	15.39	15.3	24.57
Optimized Pb (MPa)	11.70	25.42	32.02	14.58	17.28	15.39	15.29	24.59
Experimental Pb (MPa)	11.77	25.56	32.02	14.58	17.29	15.39	15.3	24.57
Initial Liq Dense@ Pb (Kg/m^3)	713.82	549.57	542.63	709.52	645.42	619.78	618.87	591.08
Matched Liq Dense@ Pb (Kg/m^3)	741.97	617.34	545.74	721.64	660.62	678.66	642.40	597.56
Optimized Liq Dense@ Pb (Kg/m^3)	795.92	626.06	545.41	721.21	657.58	672.09	665.42	586.36
Real Liq Dense@ Pb (Kg/m^3)	741.80	617.67	545.55	721.50	659.63	-	-	596.66

bubble point pressure is 18.9% with “initial” set of parameters, 0% with “matched” set of parameters, and 0.2% with “optimized” set of parameters. Although, the AAD% in the final regression has been increased to 0.2%, such deviations are completely acceptable for saturation pressure modeling. In addition, AAD% for samples 3, 4, and 6 are zero after final regression step.

In Table 10, AAD% of saturated liquid density is 3.3% with “initial” set of parameters, 0.1 with “matched” set of parameters and 1.8 with “optimized” set of parameters. This shows a behavior similar to bubble point pressure. As can be observed, the samples 1, 4, 6, and 7 show the highest deviation from the measured MMP data. One common criterion of all these four samples is that the methane mole fraction in these samples is smaller relative to the other 4 samples. The large deviations in MMP calculation prove conventional EOS regression shortcomings for the gas injection projects and MMP calculation; moreover, the large deviations in MMP calculation show the necessity of MMP regression in addition to conventional test regressions. Also, simulated-annealing algorithm for regression of the EOS parameters using the objection function constructed from the deviations from the conventional and miscible injection test data is shown in Figure 5.

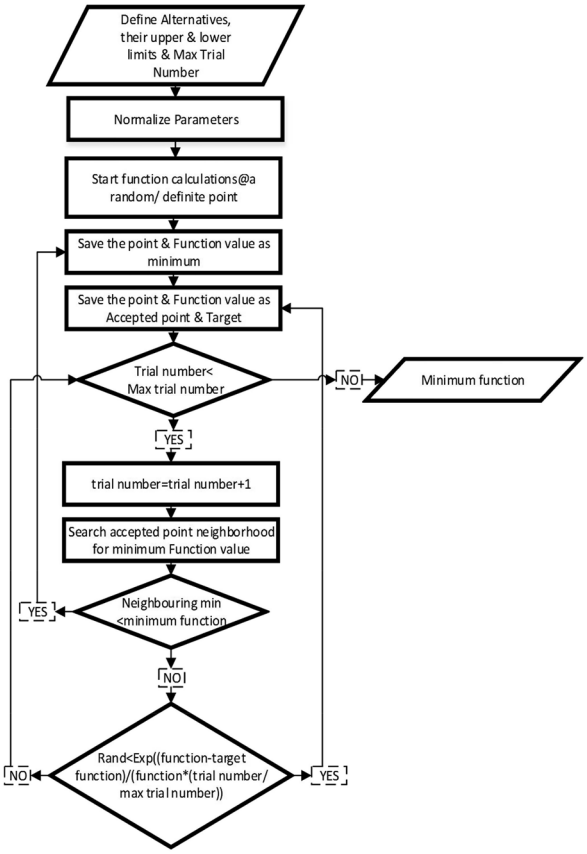

Figure 5: Simulated-Annealing algorithm for regression of the EOS parameters using the objection function constructed from the deviations from the conventional and miscible injection test data.

A discussion of the limitations and a comparison to other works can be done in two different levels:

level 1, after regression: the optimized set of parameters produce nearby zero deviation from experimental MMPs. In addition, currently, there is no automated regression tool for slim tube compositional simulation in the literature applied for MMP regression. The work in the literature for tuning the fluid model with MMP has been proposed by Negahban and Kremesec [36] and Jaubert et al [37]. They did not consider the slim tube compositional simulation (which is the simulation of a standard method to measure MMP). The limitation in this level is that, we programmed saturation pressure and liquid density to find the regression in objective function. In case, it is necessary to consider the honor more data, the complexity of regression is increased, and its success can be limited.

Level 2, before regression: MMP calculation from slim tube compositional simulation (i.e. manual calculation of MMP from the recovery factor) has been evaluated and compared in different works including the works of ([33] and [43]). The limitation of this modeling approach is the necessity to have the full characterization of reservoir oil and injected gas which makes it unsuitable for fast calculations.

CONCLUSIONS

Determining a precise MMP is necessary for a miscible injection design. The compositional simulator is one of the best numerical methods in this regard, although its accuracy depends greatly on the EOS validity. The non-unique nature of matching procedure during conventional PVT study increases uncertainty in MMP prediction. Automated and accurate modeling and regression procedure are required to use both conventional PVT and MMP data. This “EOS set of parameters” is suitable for simulation of conventional depletion and gas injection processes. One of the important aspects of this study is using real reservoir fluids for the proposed procedure evaluation. In addition, the injected gas samples were real gases. Moreover, simulated annealing algorithm was implemented to find the optimum values. This lowers the deviation of MMP and bubble point pressure simultaneously, with the desired weighing factors. The critical properties and binary interaction coefficients of the heavy fractions had significant effects on the conventional phase behavior modeling. Finally, based on the study, the critical properties and volume shifts had considerable effects on the calculated MMP in the

final regression phase, however, after preliminary regression to the conventional PVT data, the binary interaction coefficients did not have significant impacts on MMP.

NOMENCLATURES

CCE	: Constant Composition Expansion
DL	: Differential Liberation
MMP	: Minimum Miscibility Pressure
PV	: Pore Volume
PVT	: Pressure Volume Temperature
SA	: Simulated Annealing

REFERENCES

1. Ahmadi M. A., Zahedzadeh M., Shadizadeh S. R., and Abbassi R., "Connectionist Model for Predicting Minimum Gas Miscibility Pressure: Application to Gas Injection Process," *Fuel Journal*, **2015**, *148*, 202-211.
2. Gasem K. A. M., Dickson K. B., Shaver R. D., and Robinson R. L., "Experimental Phase Densities and Interfacial Tensions for a CO_2/Synthetic-Oil and a CO_2/Reservoir-Oil System," *SPE Reservoir Engineering*, **1993**, *8*(03), 170-174.
3. Yellig W. F. and Metcalfe R. S., "Determination and Prediction of CO_2 Minimum Miscibility Pressures," *Journal of Petrol Technology*, **1980**, *30*, 1-9.
4. Huang S. and Dyer B., "Miscible Displacement in the Weyburn Reservoir: A Laboratory Study," *Journal of Canadian Petroleum Technology*, **1993**, 32, 5-17.
5. Hagen S. and Kossack C. A., "Determination of Minimum Miscibility Pressure Using a High-Pressure Visual Sapphire Cell," *SPE Enhanced Oil Recovery Symposium*, Tulsa, Oklahoma, **1986**.
6. Zhou D. and Orr F. M., "An Analysis of Rising Bubble Experiments to Determine Minimum Miscibility Pressures," *SPE Journal*, **1998**, *3*, 1-7.
7. Orr Jr F. M. and Jensen C. M., "Interpretation of Pressure-Composition Phase Diagrams for CO_2/Crude-Oil Systems," *Society of Petroleum Engineers Journal*, **1984**, *24*(05), 485-497.
8. Bryant D. W. and Monger T. G., "Multiple-Contact Phase Behavior Measurement and Application With Mixtures of CO_2 and Highly Asphaltic Crude," **1988**, *3*(02), 701-710.
9. Menzie D. E. and Nielsen R. F., "A Study of the Vaporization of Crude Oil by Carbon Dioxide Repressuring," *Journal of Petroleum Technology*, **1963**, *15*(11), 1247-1253.
10. Wang Y. and Peck D. G., "Analytical Calculation of Minimum Miscibility Pressure: Comprehensive Testing and Its Application in a Quantitative Analysis of the Effect of Numerical Dispersion for Different Miscibility Development Mechanisms," *SPE/DOE Improved Oil Recovery Symposium*, Tulsa, Oklahoma, **2000**, 1-11.
11. Christiansen R. L. and Haines H. K., "Rapid Measurement of Minimum Miscibility Pressure With the Rising-Bubble Apparatus," *SPE Reservoir Engineering*, **1987**, *2*, 522-527.
12. Harmon R. A. and Grigg R. B., "Vapor-Density Measurement for Estimating Minimum Miscibility Pressure (includes associated papers 19118 and 19500)," *SPE Reservoir Engineering*, **1988**, *3*, 1-8.
13. Abedini A., Mosavat N., and Torabi F., "Determination of Minimum Miscibility Pressure of Crude Oil–CO_2 System by Oil Swelling/Extraction Test," *Energy Technology*, **2014**, *2*, 431-439.
14. Liu Y., Jiang L., Tang L., and Song Y., "Minimum Miscibility Pressure Estimation for a CO_2/n-Decane System in Porous Media by X-ray CT," *Experiments in Fluids*, **2015**, *56*, 154.

15. Liu Y., Jiang L., Song Y., and Zhao Y., "Estimation of Minimum Miscibility Pressure (MMP) of CO_2 and Liquid n-alkane Systems Using an Improved MRI Technique," *Magnetic Resonance Imaging*, **2016**, *34*, 97-104.
16. Czarnota R., Janiga D., Stopa J., and Wojnarowski P., "Determination of Minimum Miscibility Pressure for CO_2 and Oil System Using Acoustically Monitored Separator," *Journal of CO_2 Utilization*, **2017**, *17*, 32-36.
17. Zick A. A., "A Combined Condensing/Vaporizing Mechanism in the Displacement of Oil by Enriched Gases," *SPE Annual Technical Conference and Exhibition*, New Orleans, Louisiana, **1986**, 1-11.
18. Khorsandi S. and Johns R. T., "Tie-Line Solutions for MMP Calculations By Equations-of-State," *SPE Annual Technical Conference and Exhibition*, Houston, Texas, USA, **2015**.
19. Zhong Z. and Carr T. R., "Application of Mixed Kernels Function (MKF) Based Support Vector Regression Model (SVR) for CO_2-Reservoir oil Minimum Miscibility Pressure prediction," *Fuel Journal*, **2016**, *184*, 590-603.
20. Ahmadi M. A., Zendehboudi S., and James L. A., "A Reliable Strategy to Calculate Minimum Miscibility Pressure of CO_2-oil System in Miscible Gas Flooding Processes," *Fuel*, **2017**, *208*, 117-126.
21. Johns R. T. and Orr Jr. F. M., "Miscible Gas Displacement of Multicomponent Oils," *SPE Journal*, **1996**, *1*(01), 39-50.
22. Wang Y. and Orr F. M., "Analytical Calculation of Minimum Miscibility Pressure," *Journal of Fluid Phase Equilibria*, **1997**, *139*, 101-124.
23. Kanatbayev M., Meisingset K. K., and Uleberg K., "Comparison of MMP Estimation Methods with Proposed Workflow," *SPE Bergen One Day Seminar*, Bergen, Norway, **2015**.
24. Li L., Khorsandi S., Johns R. T., and Ahmadi K., "Multiple Mixing Cell Method for Three-Hydrocarbon-Phase Displacements," *SPE Improved Oil Recovery Symposium*, Tulsa, Oklahoma, USA, **2015**, *20*(06), 1-339.
25. Ahmadi K. and Johns R. T., "Multiple-Mixing-Cell Method for MMP Calculations," *SPE Journal*, **2011**, *16*(04), 733-742.
26. Rezaveisi M., Johns R. T., and Sepehrnoori K., "Application of Multiple-Mixing-Cell Method to Improve Speed and Robustness of Compositional Simulation," *SPE Journal*, **2015**, *20*(03), 565-578.
27. Teklu T. W., Alharthy N., Kazemi H., and Yin X., "Minimum Miscibility Pressure in Conventional and Unconventional Reservoirs," *Unconventional Resources Technology Conference*, **2013**, 2206-2216.
28. Teklu T. W., Ghedan S. G., Graves R. M., and Yin X., "Minimum Miscibility Pressure Determination: Modified Multiple Mixing Cell Method," *SPE EOR Conference at Oil and Gas West Asia*, Muscat, Oman, **2012**, 1-13.
29. Johns R. T., Ahmadi K., Dengen Z., and Yan M., "A Practical Method for Minimum-Miscibility-Pressure Estimation of Contaminated CO_2 Mixtures," *SPE Journal*, **2010**, *13*(05), 764-772.
30. Khorsandi Kouhanestant S., "Mathematics of Multiphase Multiphysics Transport in Porous Media," *Energy and Mineral Engineering*, The Pennsylvania State University, **2016**.
31. Metcalfe R. S., Fussell D. D., and Shelton J. L., "A Multicell Equilibrium Separation Model for the Study of Multiple Contact Miscibility in Rich-Gas Drives," *SPE Journal*, **1973**, *13*(03), 147-155.

32. Pederson K. S., Fjellerup J., Thomassen P., and Fredenslund A., "Studies of Gas Injection Into Oil Reservoirs by a Cell-to-Cell Simulation Model," *SPE Annual Technical Conference and Exhibition*, New Orleans, Louisiana, **1986**, 1-8.
33. Jaubert J. N., Wolff L., Neau E., and Avaullee L., "A Very Simple Multiple Mixing Cell Calculation To Compute the Minimum Miscibility Pressure Whatever the Displacement Mechanism," *Industrial and Engineering Chemistry Research*, **1998**, *37*, 4854-4859.
34. Yan W., Michelsen M. L., and Stenby E. H., "Calculation of Minimum Miscibility Pressure Using Fast Slimtube Simulation," *SPE Improved Oil Recovery Symposium*, Tulsa, Oklahoma, USA, **2012**, 1-16.
35. Egwuenu A. M., Johns R. T., and Li Y., "Improved Fluid Characterization for Miscible Gas Floods," *SPE Reservoir Evaluation & Engineering*, Society of Petroleum Engineers, **2008**.
36. Negahban S. and Kremesec Jr. V. J., "Development and Validation of Equation-of-State Fluid Descriptions for CO_2/Reservoir-Oil Systems," **1992**, 1-16.
37. Jaubert J. N., Avaullee L., and Pierre C., "Is It Still Necessary to Measure the Minimum Miscibility Pressure?," *Industrial and Engineering Chemistry Research*, **2002**, *41*, 303-310.
38. Amao A. M., Siddiqui S., and Menouar H., "A New Look at the Minimum Miscibility Pressure (MMP) Determination from Slimtube Measurements," *SPE Improved Oil Recovery Symposium*, Tulsa, Oklahoma, USA, **2012**.
39. Emanuel A. S., Behrens R. A., and McMillen T. J., "A Generalized Method for Predicting Gas/Oil Miscibility," *SPE Journal,* **1986**, *1*(05), 463-473.
40. Peng D. Y. and Robinson D. B., "A New Two-Constant Equation of State," *Industrial and Engineering Chemistry Fundamentals*, **1976**, *15*, 59-64.
41. Jaubert J. N., Avaullee L., and Souvay J. F., "A Crude Oil Data Bank Containing more than 5000 PVT and Gas Injection Data," *Journal of Petroleum Science and Engineering*, **2002**, *34*, 65-107.
42. Assareh M., Pishvaie M. R., Ghotbi C., and Mittermeir G. M., "Development of a New Workflow for Pseudo-component Generation of Reservoir Fluid Detailed Analysis: A Gas Condensate Case Study," *International Journal of Oil, Gas, and Coal Technology*, **2014**, *7*, 275-297.
43. Kesler M. G. and Lee B. I., "Improve Prediction of Enthalpy Fractions," *Hydrocarbon Processing, International Edition,* **1976**, *55*, 153-158·
44. Whitson C. H., "Topics on: Phase Behaviour and Flow of Petroleum Reservoir Fluids," Doctoral Thesis, Department of Petroleum and Chemical Engineering, The University of Trondheim, Norwegian Institute of Technology, **1983**.
45. Lohrenz J., Bray B. G., and Clark C. R., "Calculating Viscosities of Reservoir Fluids From Their Compositions," *Journal of Petroleum Technology*, **1964**, *16*(10), 1-171.
46. Jhaveri B. S. and Youngren G. K., "Three-Parameter Modification of the Peng-Robinson Equation of State To Improve Volumetric Predictions," *SPE Reservoir Engineering*, **1988**, *3*(03), 1-33.